Environ. Eng. Res. 2018; 23(2): 216-222
https://doi.org/10.4491/eer.2017.193

pISSN 1226-1025
eISSN 2005-968X

Quantitative analysis of *Spirulina platensis* growth with CO_2 mixed aeration

Yong Sang Kim[1*], Sang-Hun Lee[2*†]

[1]*Water and Environmental Research Institute of the Western Pacific, University of Guam, Mangilao, Guam 96923, USA*
[2]*Department of Environmental Sciences, Keimyung University, Daegu 42601, Republic of Korea*
**These authors contributed equally to this work.*

ABSTRACT

The growth characteristics of *Spirulina platensis* were investigated using four photo-bioreactors with CO_2-mixed air flows. Each reactor was operated under a specific condition: 3% CO_2 at 50 mL/min, 3% CO_2 at 150 mL/min, 6% CO_2 at 50 mL/min, and 6% CO_2 at 150 mL/min. The 3% CO_2 at 150 mL/min condition produced the highest algal growth rate, while the 6% CO_2 at 150 mL/min conditioned produced the lowest. The algal growth performance was suitably assessed by the linear growth curve rather than the exponential growth. The medium pH decreased from 9.5 to 8.7-8.8 (3% CO_2) and 8.4-8.5 (6% CO_2), of which trends were predicted only by the pH-carbonate equilibrium and the reaction kinetics between dissolved CO_2 and HCO_3^-. Based on the stoichiometry between the nutrient amounts and cell elements, it was predicted that depleted nitrogen (N) at the early stage of the cultivation would reduce the algal growth rates due to nutrient starvation. In this study, use of the photobioreactors capable of good light energy distribution, proper ranges of CO_2 in bubbles and medium pH facilitated production of high amounts of algal biomass despite N limitation.

Keywords: Algae, pH-carbonate system, Nitrogen (N) limitation, Photo-bioreactor, *Spirulina platensis*

1. Introduction

As highlighted by the Inter-government Panel on Climate Change (IPCC) in 1988, Kyoto Protocol in 1997 [1] and the Paris Agreement in 2015, reducing greenhouse gases is a global concern. The 17th Conference of the Parties (COP) held in 2011 in Durban, South Africa, focused on finding ways to reduce greenhouse gases and the COP adopted the Durban Outcome [2]. According to the outcome, all member countries of UNFCC have to take action towards reducing global warming gases beginning in 2020. Greenhouse gases that trigger global warming include carbon dioxide (CO_2), methane (CH_4), nitrous oxide (N_2O), hydrofluorocarbons (HFCs), perfluorocarbons (PFCs), and sulfur hexafluoride (SF_6). The focus of attention has been mainly on reduction of CO_2 because this gas forms the majority of emissions [3].

One promising CO_2 reduction technology is the use of photosynthetic microorganisms, whose CO_2 fixation efficiency can be increased quite simply using a highly concentrated microbial population [4]. The compelling advantages of this technique include the ease of algae in adapting to new environments, simple population growth [5-6], and the abundance of proteins, carbohydrates, and nutrients in the algal biomass that develops during microbial growth through CO_2 fixation [4, 6-7]; the resulting biomass can be recovered and utilized as an alternative food or energy source [3, 6-8]. In addition, algal biomass can acts as adsorbent to purify water by toxic metal adsorption [9]. CO_2 fixation using photosynthetic microalgae has become a very attractive potential approach to resolve global issues of energy as well as simultaneously increasing the global food supply and water purification.

Spirulina platensis (*S. platensis*) is a promising microalga for CO_2 fixation because of its rapid population growth and production of valuable compounds with a high percentage of proteins, vitamins, and g-linolenic acid [6]. Many studies have addressed the mass production of microalgae in regions that receive high levels of direct sunlight and have a high ambient air temperature. Recently, there has been growing interest in photoautotrophic algal reactors that are engineered for enhanced production rates [3, 6, 10-11].

Received November 26, 2017 **Accepted** February 1, 2018

† Corresponding author
Email: shlee73@kmu.ac.kr
Tel: +82-53-580-5912
ORCID: 0000-0003-2577-1736

Many researchers have focused on experimental observations to identify the correlation between key factors and algal cultivation, or to identify optimal algal growth conditions [3, 6, 10-15]. Increased algal production attenuates light capacity, which in turn affects growth rates, making any increased production self-limiting in nature [14]. CO_2 and nutrient concentrations are also significant parameters [3, 5, 7-8, 12-20]. In particular, dissolution of CO_2 governs pH, which will eventually affect algae levels. However, there is a lack of mechanistic and quantitative analyses of algae biomass concentrations, nutrients, and pH associated with CO_2-mixed air flows. All these factors should all be considered to optimize algae production.

In this study, the growth characteristics of *S. platensis* were investigated using four cylindrical 400-mL photo-bioreactors with CO_2-mixed air gas flows. Each reactor was operated under a given flow condition: 3% CO_2 at 50 mL/min, 3% CO_2 at 150 mL/min, 6% CO_2 at 50 mL/min, and 6% CO_2 at 150 mL/min. This study further improved the authors' previous study [21]. The analyses include regression fitting for the algal growth curves, prediction of pH in medium using the reaction equilibrium and kinetics, and stoichiometric assessment of nitrogen (N) limitation.

2. Materials and Methods

2.1. Materials

S. platensis UTEX LB 2340 was obtained from the University of Texas at Austin. The culture medium was alkaline inorganic. The components included $NaHCO_3$ (13.61 g/L), Na_2CO_3 (4.03 g/L), K_2HPO_4 (0.50 g/L), $NaNO_3$ (2.50 g/L), K_2SO_4 (1.00 g/L), NaCl (1.00 g/L), $MgSO_4 \cdot 7H_2O$ (0.20 g/L), $CaCl_2 \cdot 2H_2O$ (0.04 g/L), PIV metal solution (6 mL/L), Chu micronutrient solution (1 mL/L), and Vitamin B_{12} (1 mg/1000 mL H_2O; 150 mL/L). The PIV metal solution consisted of Na_2EDTA (750 mg/L), $MnCl_2 \cdot 4H_2O$ (41.2 mg/L), $CoCl_2 \cdot 6H_2O$ (2.0 mg/L), $Na_2MoO_4 \cdot 2H_2O$ (4.0 mg/L), $FeCl_3 \cdot 6H_2O$ (97.2 mg/L), and $ZnCl_2$ (5.2 mg/L). The components of Chu micronutrient solution included Na_2EDTA (750 mg/L), $MnCl_2 \cdot 4H_2O$ (12.8 mg/L), $CoCl_2 \cdot 6H_2O$ (20.0 mg/L), $Na_2MoO_4 \cdot 2H_2O$ (12.8 mg/L), H_3BO_3 (618.0 mg/L), $CuSO_4 \cdot 5H_2O$ (19.6 mg/L), and $ZnSO_4 \cdot 7H_2O$ (44.0 mg/L). The medium was utilized for cultivation after being sterilized at 121℃ for 15 min in a high-pressure sterilizer. Algae were cultivated in a 250-mL Erlenmeyer flask with stirring at 120 rpm for 12 h under light and 12 h in darkness. The initial pH and temperature of the medium was 9.5 and 30℃, respectively. The light was provided by a 25 mmol/m^2-s fluorescent lamp. For algae growth, 400 mL of inoculated medium was prepared using sterilized medium and 0.1 g/L (dry condition) *S. platensis*. The inoculant medium was injected into the reactor, which had been sterilized beforehand.

2.2. Photoreactors

The cylindrical photoautotrophic bioreactor had a diameter of 4 cm, depth of 65 cm, and volume of 400 mL. The CO_2/air mixture was supplied using an air pump and a gas mixer. To prevent contamination by dust or microbes, a 0.2-mm filter was installed at the gas inlet of each reactor. Identical spargers were installed inside the reactor so that microbubbles of CO_2 in air could be effectively transferred to the medium. Fluorescent lamps were installed along each side of the reactor. Fig. 1 shows the reactor set-up. The test parameters to investigate the effects of CO_2 concentration and air- mixture flow rates were 3% CO_2 at 50 mL/min, 3% CO_2 at 150 mL/min, 6% CO_2 at 50 mL/min, and 6% CO_2 at 150 mL/min. The pH of the medium immediately after inoculation was 9.5, and reaction temperature was maintained at 30℃ using a water circulator. Light intensity was consistent at 110 mmol/m^2-s.

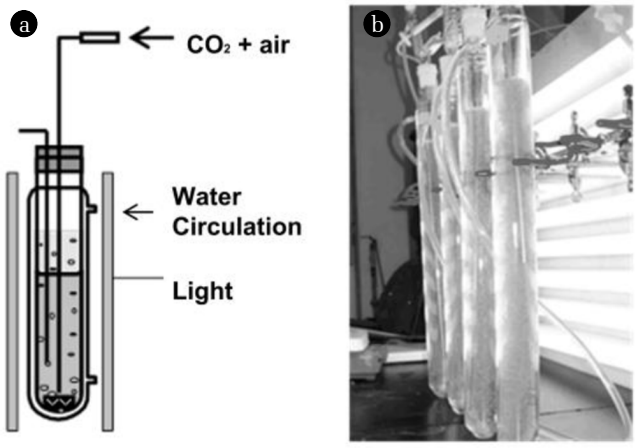

Fig. 1. Cylindrical photo-bioreactor for culturing *S. platensis*. (a) schematic and (b) photograph. Modified from Kim *et al*. [21].

2.3. Analytical Techniques

The amount of microalgal biomass concentration (cell population density) was obtained by measurement of the optical density (O.D.) at 670 nm using a model U-2000 UV spectrophotometer (Hitachi, Chiba, Japan). The dry biomass (= −0.4289×O.D.) was confirmed to have a good linear correlation (r^2~99%) with the O.D. The similar analysis to determine cell growth was utilized by Chen *et al.* and Xie *et al.* [10-11]. The pH of the medium was measured using a model HI8424 pH meter (Hanna Instruments, Woonsocket, RI, USA). The initial concentrations of N and phosphate (P) in the medium were 305.0 mg/L (NO_3-N) and 73.0 mg/L (PO_4-P) as measured by ion chromatography (IC) using a DX-120 apparatus (Dionex, Sunnyvale, CA, USA).

2.4. Data Analysis

The exponential and linear regression curves were provided to characterize the dynamic growth curves for each reaction set. The coefficient of determination was found for each curve to assess the fit in the regressions to the corresponding experimental data. Also, Analysis of Variance (ANOVA) was performed with the regression parameters to compare the dynamic algal growth between individual reaction set. If any regression of a data set could not properly characterize a dynamic curve, the data set would undergo a simple treatment (such as geometric averaging) and then conduct the multiple comparison. The regression and the comparative statistical analysis were implemented using MS-Excel and R software.

3. Results and Discussion

The dynamic cell-growth curves and their regression fits on *S. platensis* and the dynamic variation of medium pH are shown in Fig. 2. The highest algal biomass concentration and growth curve were obtained for 3% CO_2 at 150 mL/min. The 6% CO_2 at 150 mL/min condition produced a similar growth pattern, while 6% CO_2 at 50 mL/min yielded the lowest growth. Interestingly, both sets with a flow rate of 150 mL/min showed higher *S. platensis* growth than their counterparts with a flow rate of 50 mL/min. The similar trend of the influences of CO_2 contents or aeration flow rates to the algal growth was observed in the previous studies [12-13].

With the respect to the model fits, the early phase of the algal growth in Fig. 2 was characterized by conventional exponential growth until 134 h, in which the increase of the algal population (dX/dt) has normally assumed to have been proportional to the concentration of the algal biomass concentrations (X) [3, 14]. The specific growth rate in the exponential growth can be simply calculated as $(\ln X_2 - \ln X_1)/(t_2 - t_1)$, by applying an ordinary differential equation (ODE) solving technique of the separation of variables. However, a linear increase of biomass concentration predominated in mid-to-final stages of the cultivations (144-332 h). In this study, linear growth rate was described using the model presented by Ogbonna *et al.* [14]. The model was constructed with the assumption that the growth rate is proportional to the maximum total light energy absorbed in a reactor divided by the liquid volume of the reactor. Here, the constant specific growth rate of the original exponential growth ($dX/dt = mX$) is modified to be a function that is inversely proportional to the biomass population concentrations X ($dX/dt = K_{aL}$). It is quite reasonable for the case of absorbed light energy limited by concentrated biomass produced.

The pH of each condition differed significantly according to the CO_2 concentration of the gas in the bubbles, regardless of the gas flow rates. At the beginning of the experiment, the pH was 9.5. By 20 h and thereafter, the pH stabilized at 8.8 ± 0.2 for 3% CO_2 and 8.5 ± 0.2 for 6% CO_2 as similar to the previous studies [3, 10, 12].

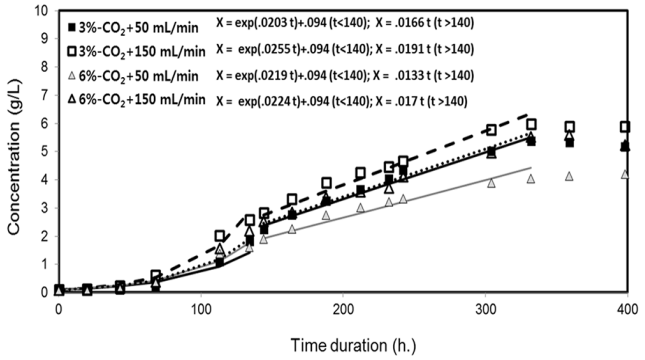

Fig. 2. The mode fits with the exponential and the regressions to the experimental data on dynamic variation of algal biomass concentrations.

Fig. 2 includes the exponential (0-134 h) and the linear regressions for reaction times from 144-332 h. The linear regression equations were included in a range of 0.0138-0.0191 /h, while the constants were different according to the reactor sets. The condition of 3% CO_2 at 150 mL/min had the highest linear growth rate.

$$K_{aL} = -10^{6.13} \times 10^{-pH} + 10^{-4.24} \times Q_a + 0.017 \ (R^2 > 93\%) \quad (1)$$

Here, K_{aL} represents the parameter of the linear growth rate; *pH* represents the stabilized pH of the solution medium, and Q_a denotes the aeration rate. Each growth rate could be well described by linear curves with the coefficients of determination greater than 93%. Based on ANOVA analysis with the F statistic with each linear coefficient, there is a higher significance ($p \approx 0.10$) of difference between the individual linear curves with respect to the aeration rates than CO_2 levels ($p \approx 0.14$). This means the aeration rates can be an effective factor to differentiate the growth curves. Prior to the linear increases until 134 h, the algal growth was assumed to be described by exponential growth curves. The specific growth rates in the exponential growth rates were calculated as 0.02-0.0255/h. However, the specific growth rates had little correlation with the performance of the cultivation of individual sets. This is similar to the results of the linearity shown in many previous studies [3, 6, 13-14]. Ogbonna *et al.* reported good correlation between the linear growth rates and the final cell concentrations during light-limited batch cultivation of *Chlorella pyrenoidosa* C-212 and *S. platensis* M-135 cells, regardless of the type and size of photobioreactor [14].

3.1. pH of the Solution Media

CO_2 transferred from the gas to water phases reduces pH by formation of H_2CO_3, but the H_2CO_3 is transformed to HCO_3^- or CO_3^{2-} at pH 8-9 and pH 10-11, respectively. In this study, additional CO_3^{2-} or HCO_3^- ions were initially supplied in the medium with spontaneous dissolution of $NaHCO_3^-$ and Na_2CO_3. For that reason, the initial pH was specified as 9.5 by the equilibrium between HCO_3^- from $NaHCO_3$, and CO_3^{2-} from Na_2CO_3. According to the previous studies by James *et al.*, Martis *et al.* and Stumm and Morgan [7, 15-16], the equilibrium constant ($[H^+][HCO_3^-]/[CO_3^{2-}]$) of the reaction between the two ionic compounds HCO_3^- and CO_3^{2-} is $10^{-10.3}$ at a water temperature of 30°C. This means that at pH 10.3 the two ions have identical concentrations.

The initial pH (~9.5) should rapidly decrease because of the injection of aeration bubbles containing 3% or 6% CO_2 gas, which dissolves and is partly transformed to carbonic acid (H_2CO_3). According to Henry's constant [18], the dissolved CO_2 concentration is linearly correlated with atmospheric CO_2. Therefore, 6% CO_2 can generate twice the amount of dissolved CO_2 in the aqueous medium (≈ 1.1 mM) than 3% CO_2 (≈ 0.55 mM) at equilibrium. This is reasonable because other kinds of reactions that feature autotrophic CO_2 consumption should be slow at the beginning of the cultivation. H_2CO_3 is again transformed to HCO_3^- (> 95%) at pH < 8.5, and

HCO_3^- is the dominant carbonate species at that pH range. In addition, most of the initial CO_3^{2-} compounds combine with H^+ of H_2CO_3 to form HCO_3^-. Under the condition of sufficient C as well as the beginning of the reaction, it is reasonable that the gaseous and dissolved CO_2 (without H_2CO_3) should maintain the equilibrium.

Some CO_3^{2-} and HCO_3^- ions that exist in the medium may be acidified by H^+ in H_2CO_3, while the dissolved CO_2 is converted to HCO_3^- (through H_2CO_3). According to the kinetics of the reaction has been described in a previous study [16], more HCO_3^- is transformed to CO_2 and OH^- than its reverse conversion ($CO_2 + OH^- \rightarrow HCO_3^-$) until pH > 8.9 and pH > 8.6, for 3% CO_2 and 6% CO_2, respectively. At $CO_2 \approx 0.55$ mM (3% CO_2 set) and $CO_2 \approx 1.1$ mM (6% CO_2 set), those transformations stop around pH 8.9 and 8.6, respectively. Termination of pH drop may result not only from activation of the reverse conversion due to increase of dissolved CO_2 levels, but also from the charge balance because of the presence of enormous amounts of metal cations (mainly Na^+) dissociated from $NaHCO_3^-$ and Na_2CO_3, leading to suppress new H^+ generation. The mechanism of pH by carbonate and pH is illustrated in Fig. 3.

Typically, algal growth accompanies consumption of CO_2, HCO_3^-, and nutrients, as well as the production of O_2 and changes in pH. As for *S. platensis*, Cornet *et al.* suggested the following stoichiometric equation [17]:

$$HCO_3^- + 0.724\ H_2O + 0.170\ NO_3^- + 0.007\ SO_4^{2-} + 0.006\ HPO_4^{2-} + 0.196H^+ \rightarrow CH_{1.650}\ O_{0.531}\ N_{0.171}\ S_{0.07}\ P_{0.006} + 1.378\ O_2 + OH^- \quad (2)$$

where $CH_{1.650}\ O_{0.531}\ N_{0.171}\ S_{0.07}\ P_{0.006}$ is a typical element composition of *S. platensis*. Compared with the old one, there is a different cell composition of *S. platensis*, recently suggested by da Silva *et al.* [6].

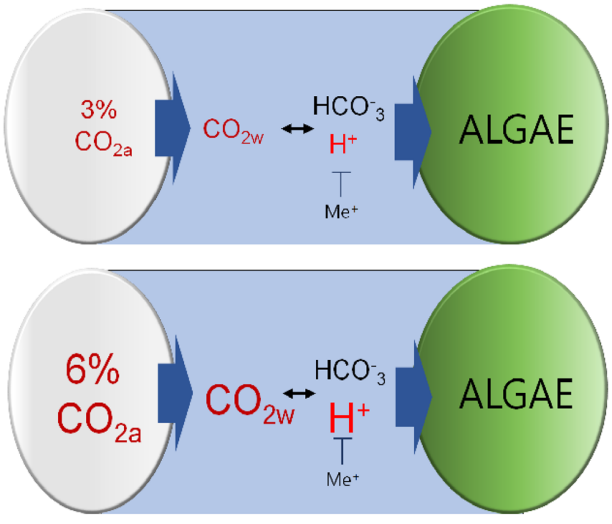

Fig. 3. Schematic demonstration of the carbonate-pH equilibrium and kinetics; pH stabilized by dissolved CO_2 decreasing pH which is however suppressed by conversion to HCO_3^- and by charge balance with cations (Na^+).

$$HCO_3^- + 0.1\ NO_3^- + 1.1\ H^+ \rightarrow CH_{1.65}\ O_{0.5}\ N_{0.1} + 1.272\ O_2 + 0.255\ H_2O \quad (3)$$

Eq. (2)-(3) indicates both the metabolic reactions consume H^+ and/or produce OH^- leading to a potential pH increase, but becomes neutralized by the aforementioned H^+ produced by CO_2 supplied in the injected aeration bubbles. As a result, rather stable pH levels were maintained over the whole reaction. It has been reported that the optimal pH for biomass production of *S. platensis* should be around 9.0-9.5, and the amount of biomass decreases as the pH decreases at 30°C if no additional control was made [10, 12]. The present finding of different biomass production with pH supports those of a previous study [13]; the low pH from 6% CO_2 should be more disadvantageous for *S. platensis* growth than that of the 3% CO_2 condition. Several studies have described decreased growth of *S. platensis* by high CO_2 in aeration, leading to decreased pH of the medium [3, 12-13]. Park *et al.* study commented that the high CO_2 supply accelerated the growth rates but eventually obtained lower cell biomass concentrations [3].

3.2. Influences of Aeration Rates

There have been few studies on the effects of aeration and gas flow rate on the growth of *S. platensis*. Tadros showed that algal growth increased with increasing aeration rates in the range of 150-500 mL/min, although growth was deterred at a high aeration rate of 2,000 mL/min [12]. Why aeration affects algal growth remains unclear. The most plausible explanation is the facilitated mass transfer of CO_2 from air to algal biomass, but this does not explain the present results, since pH was stable all during growth. Furthermore, pH was more strongly affected by CO_2 in the bubbles than the aeration rates. CO_2 was not appreciably affected by the rate of aeration. This implies that CO_2 mass transfer from the bubbles to the medium should be far greater than CO_2 consumption by algae at the beginning of algal growth. Thus, the stable pH is due to the CO_2 consumption rate, which remains lower than CO_2 mass transfer regardless of CO_2 concentration for high algal biomass. The advantages of increased aeration rates may actually result from deformation of microbubbles at high flow rates, leading to improved mass transfer of gases other than CO_2, homogeneous mixing of nutrients, or promoted light distribution into individual cells by the mixing.

3.3. Influence of N and P Concentration in Dynamic Cell Growth

Fig. 4 shows NO_3-N (Fig. 4(a)) and PO_4-P (Fig. 4(b)) concentrations measured in the media at 0, 113, 212, and 398 h. The residual N concentrations at these times were 40-60%, 3-7%, and 0%, respectively, of the initial N concentration for all reaction conditions. In contrast to the huge drop in the residual N concentrations in the middle hours of the cultivation, PO_4-P levels gradually decreased, with a loss of only 10-20% at 113 h and ~50% at 212 h. Even at 398 h, about 20-30% of the initial P level remained in the media for all reaction conditions. Like N removal, the conditions of 3% CO_2 at 150 mL/min and 6% CO_2 at 50 mL/min yielded the lowest and highest P concentrations, respectively, at 113 h.

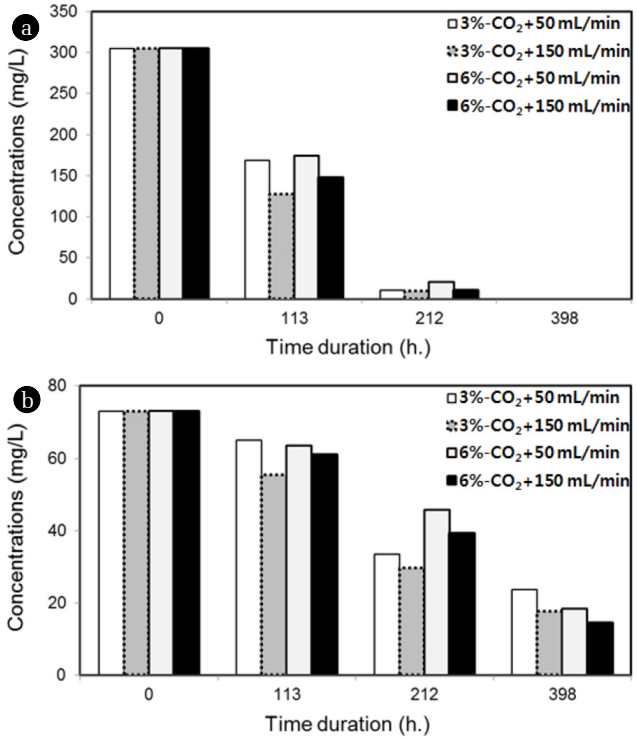

Fig. 4. Residual N (a) and P (b) concentrations in culture media during growth of *S. platensis*.

The residual N and P concentrations in Fig. 4(a)-4(b) were compared using ANOVA according to individual sets. The N concentrations on 113 h and 212 h in Fig. 4(a) were averaged for each set to obtain their geometrical means, and produced F-statistic to assess if there are significance of differences according to aeration rates or CO_2 concentrations. Similarly, the P concentrations on 113 h, 212 h and 398 h in Fig. 4(b) were utilized for the ANOVA through the geometrical averaging. As a result, the P concentrations exhibited a marginal significance of difference ($p \approx 0.08$) according to aeration rates while other cases (the N concentrations for both sets and the P concentrations with CO_2 levels) showed no significance of difference. The P consumption corresponded the trend of cell growth in that both produced the higher significance of differences for the aeration rates than CO_2 levels. In contrast, the insignificance of difference in the N concentrations regardless of sets noted that the algal N consumption had little dependence on aeration rates or CO_2 levels; another mechanism should be dominant for N consumption.

This study performed a stoichiometric analysis to predict nutrient starvation during growth of *S. platensis*, based on the presumption that the N consumption was derived by N deficit of nutrient starvation. Nutrient starvation occurs when the available nutrients are much less than the required amounts for algal growth. It is assumed that the required quantities of the nutrients can be determined from a typical elemental composition of *S. platensis* ($CH_{1.650}\ O_{0.531}\ N_{0.171}\ S_{0.07}\ P_{0.006}$ and $CH_{1.65}\ O_{0.5}\ N_{0.1}$), as shown in Eq. (2)-(3), respectively. The weight ratio of N in

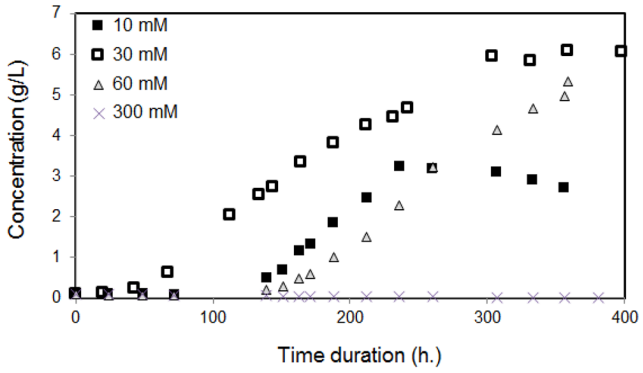

Fig. 5. Experimental dynamic variation of *S. platensis* biomass concentrations according to various initial N concentrations.

S. platensis was 8.0% with C:N ratio of 5:1 based on the elemental composition in Eq. (2), while the respective 6% and 8.6:1 of the weight and C:N ratios in Eq. (3). The former one is similar to the result of a previous study measuring C:N ratio of 5.5:1 with N sufficiency, while the latter one is close to the case of N deficiency [13].

Even if the stoichiometric model in this study presumed that the algal growth should terminated when nutrient N is exhausted, decreased N composition inside the algal biomass by down-regulating intensive N metabolism reduced the N consumption as available N was exhausted in the culture media [3, 13]. These studies confirmed that the algal growth we observed could be continued by changing the composition of the algal biomass even after the available N had been exhausted. This explains why the algal growth could be sustained even after the N was almost exhausted in the middle of the culture growth.

To further investigate the N effects to algal growth, the biomass concentrations were measured according to the various initial $NaNO_3$-N concentrations in the culture medium. Fig. 5 presents the resultant data; the initial N concentrations of 30 mM and 60 mM proved favorable for algal growth. In contrast, 10 mM and 300 mM resulted in premature decline in growth because of lacks of N at the lower concentration and inhibition of growth by the excessively high N. This is entirely consistent with prior findings; even though N is an essential nutrient for algal growth, excessive concentrations restrict algal growth [11, 12]. In the case of P consumption as well as the relevant cell composition in Eq. (2), the quantity of P was relatively sufficient until the end of the growth experiment, P probably must not act as the source of nutrient limitation.

3.4. Performance of the Process

The final biomass concentrations were far higher than in many previous studies with the lab-scaled photoreaction with *S. platensis* [3, 5, 13, 19]. The biomass concentrations ranged 1-3 g/L which is far lower than this present study with 4-6 g/L. Gordillo *et al.* [13] obtained low biomass concentrations probably because of the low temperature of the medium (25℃) and use of conventional Plexiglas cylinders as photobioreactor. Kim *et al.* [5] limited the photoreaction by applying a 16 h light/8 h dark photoperiod. Kumari *et al.* [19] utilized a special reactor

of CO_2-agitated sintered disk chromatographic glass bubble column with very high CO_2 contents (20-100%). The reactor system may enhance the mass transfer of CO_2, but too much high CO_2 supply and possible light inhibition in the bubble column may reduce the biomass growth. Park *et al.* [3] utilized multiple 2 L Erlenmeyer flasks with distant light sources which might be disadvantageous in algal growth, compared to a single reactor with a close light source.

In contrast, the biomass amounts obtained in Chen *et al.* [10], Cruz-Martínez *et al.* [20], da Silva *et al.* [6] and Xie *et al.* [11] produced comparable to or higher than those in this study. There is no definite clue but they possibly achieved such high biomass concentrations as well as high growth rates by using small diameters of reactors, which could both provide a favorable condition for light energy distribution through the reactor. Especially, da Silva *et al.* accomplished the biomass production up to 9 g/L with increasing Surface-to-Volume (S/V) ratio in the reactor configuration. This study also incorporated the small diameter of photobioreactor (~4 cm), which maintained high light energy incidence to obtain the high biomass concentrations.

4. Conclusions

Dynamic growth characteristics of *S. platensis* were investigated under CO_2-mixed air flows. Each reactor was operated under a given air flow condition: 3% CO_2 at 50 mL/min, 3% CO_2 at 150 mL/min, 6% CO_2 at 50 mL/min, and 6% CO_2 at 150 mL/min. The high gas flow rate of 150 mL/min and the low CO_2 content of 3% in aeration yielded high algal growth. The linear growth curves after the exponential growth type properly described the algal growth during active growth, and confirmed the good correlation with the final biomass. A deficit of N might occur after 188 h or more, leading to starvation conditions. Using the stoichiometry between the nutrient amounts and cell elements, it was predicted that depletion of N occurred in the middle of the cultivation but algal growth continued due to change of cell components to reduce N consumption. Based on the pH-carbonate equilibrium and kinetics between dissolved CO_2 and HCO_3^-, the medium pH decreased from 9.5 to 8.7-8.8 (3% CO_2) and 8.4-8.5 (6% CO_2). The photobioreactors with the small diameter (~4 cm), which allowed favorable light energy distribution, and provision of an acceptable range of CO_2 contents (3%) in bubbles as well as proper temperature and medium pH (8.7-9.8) facilitated the accumulation of high biomass concentrations in N-limited conditions.

References

1. UNFCC. Kyoto protocol; 1997.
2. United Nations. United Nations Climate Change Conference (COP17/CMP7). Durban, South Africa; 2011.
3. Park YI, Labrecque M, Lavoie JM. Influence of elevated CO_2 and municipal wastewater feed on the productivity, morphology, and chemical composition of *Arthrospira* (*Spirulina*) *platensis*. *ACS Sust. Chem. Eng.* 2013;1:1348-1356.
4. Ji MK, Abou-Shanab RAI, Kim SH, et al. Cultivation of microalgae species in tertiary municipal wastewater supplemented with CO_2 for nutrient removal and biomass production. *Eco. Eng.* 2013;58:142-148.
5. Kim K, Choi J, Ji Y, et al. Impact of bubble size on growth and CO_2 uptake of *Arthrospira* (*Spirulina*) *platensis* KMMCC CY-007. *Bioresour. Technol.* 2014;170:310-315.
6. da Silver MF, Casazza AA, Ferrari PF, et al. A new bioenergetic and thermodynamic approach to batch photoautotrophic growth of *Arthrospira* (*Spirulina*) *platensis* in different photobioreactors and under different light conditions. *Bioresour. Technol.* 2016;207:220-228.
7. Martis RV, Singh R, Ankita SK, Pathak AK, Guria C. Solubility of carbon dioxide using aqueous NPK 10:26:26 complex fertilizer culture medium and *Spirulina platensis* suspension. *J. Environ. Chem. Eng.* 2013;1:1245-1251.
8. Ji C, Wang J, Li R, Liu T. Modeling of carbon dioxide mass transfer behavior in attached cultivation photobioreactor using the analysis of the pH profiles. *Bioprocess Biosyst. Eng.* 2017;40:1079-1090.
9. Solisio C, Lodi A, Finocchio E. Effects of pH on chromate(VI) adsorption by *Spirulina platensis* biomass: Batch tests and FT-IR studies. *Water Sci. Technol.* 2013;67:1916-1922.
10. Chen CY, Kao PC, Tan CH, et al. Using an innovative pH-stat CO_2 feeding strategy to enhance cell growth and C-phycocyanin production from *Spirulina platensis*. *Biochem. Eng. J.* 2016;112:78-85.
11. Xie Y, Jin Y, Zeng X, Chen J, Lu Y, Jing K. Fed-batch strategy for enhancing cell growth and C-phycocyanin production of *Arthrospira* (*Spirulina*) *platensis* under phototrophic cultivation. *Bioresour. Technol.* 2015;180:281-287.
12. Tadros MG. Characterization of *Spirulina* biomass for CELSS diet potential. NASA Contractor NCC 2-501, USA; 1988.
13. Gordillo FJL, Jimenez C, Figueroa FL, Niell FX. Effects of increased atmospheric CO_2 and N supply on photosynthesis, growth and cell composition of the cyanobacterium *Spirulina platensis* (*Arthrospira*). *J. Appl. Phycol.* 1999;10:461-469.
14. Ogbonna JC, Yada H, Tanaka H. Kinetic study on light-limited batch cultivation. *J. Ferment. Bioeng.* 1995;80:259-264.
15. James SC, Janardhanam V, Hanson DT. Simulating pH effects in an algal-growth hydrodynamics model. *J. Phycol.* 2013;49:608-615.
16. Stumm W, Morgan JJ. Aquatic chemistry: Chemical equilibria and rates in natural waters. 3rd ed. USA: John Willey and Sons Inc.; 1996. p. 370-398.
17. Cornet JF, Dussap CG, Cluzel P, Dubertret GA. Structured model for simulation of cultures of the cyanobacterium *Spirulina platensis* in photobioreactors: II. Identification of kinetic parameters under light and mineral limitations. *Biotechnol. Bioeng.* 1992;40:826-834.
18. Sander R. Compilation of Henry's law constants (version 4.0) for water as solvent. *Atmos. Chem. Phys.* 2015;15:4399-4981.
19. Kumari A, Kumar A, Pathak AK, Guria C. Carbon dioxide assisted *Spirulina platensis* cultivation using NPK-10:26:26 complex fertilizer in sintered disk chromatographic glass

bubble column. *J. CO_2 Util.* 2014;8:49-59.
20. Cruz-Martínez LC, Jesus CKC, Matsudo MC, Danesi EDG, Sato S, Carvalho JCM. Growth and composition of *Arthrospira* (*Spirulina*) *Platensis* in a tubular photobioreactor using ammonium nitrate as the nitrogen source in a fed-batch process. *Braz. J. Chem. Eng.* 2015;32:347-356.
21. Kim YS, Park HI, Park DW. The growth characteristics of *Spirulina platensis* at different carbon dioxide concentration and flow rate. Proceedings of KSEE (Korean Society of Environmental Engineers) conference. Spring; 2003.